Hydrothermal systems

Akinfiev[1] N.N., Plyasunov [2]A. V. On the problems of calculating the solubility of metal oxides in the vapor phase of water

[1]Institute of Geology of Ore Deposits, Petrography, Mineralogy, and Geochemistry, RAS, Moscow
[2]Institute of Experimental Mineralogy, RAS, Chernogolovka
akinfiev@igem.ru

In the metal oxide-water systems available thermodynamic data for gaseous hydroxides predict the vapor phase solubility values, which are several orders of magnitude lower than the experimental determinations. An approach to solving this problem by incorporating the quantum-chemical calculations of the hydrated form of gaseous hydroxides is proposed.

Key words: solubility, quantum-chemical calculations, the thermodynamic properties of the ideal gas

Reference: Akinfiev, N. N., A. V. Plyasunov (2012), On the problems of calculating the solubility of metal oxides in the vapor phase of water, *Vestnik ONZ RAS, 4,*

A number of investigators on the basis of studies of gas-liquid inclusions, analyzes of fumarolic gas condensates and experimental studies have shown that the vapor phase of hydrothermal solutions is able to transfer significant amounts of metalloids (B, Si, Ge, As, Sb, Te, etc.) and even metals (Mo, Ag, Cu, Au). Available to geochemists thermodynamic databases do not allow to predict the behavior of these metals in the low-density fluids with sufficient accuracy. Thus, the determination of the speciation of the elements in the vapor phase and their thermodynamic properties is an important task of modern geochemistry of hydrothermal processes.

The analysis should begin with those forms, which always exist in the presence of water, i.e. with the oxide and hydroxide species. For a number of metalloids the stoichiometry of the species have been determined spectroscopically – these are hydroxides (i.e. $As(OH)_3$, $B(OH)_3$, $Si(OH)_4$, etc.).

The thermodynamics allows calculating the values of the solubility of oxides in steam, if the thermodynamic properties of the hydroxides in the ideal gas state and their fugacity coefficients $\phi_2^\infty(T,\ P)$ as a function of temperature and pressure are known. For the dissolution reaction $MeO(s) + nH_2O(g) = MeO\cdot(H_2O)_n(g)$ at given T и P the following expression for the equilibrium constant is valid:

$$\ln K^{o}(T) = \ln \frac{Y_2 \cdot (P/P^{\otimes})\phi_2^{\infty}}{(f_1)^n} - \frac{V(\mathrm{MeO(s)}) \cdot (P - P^{\otimes})}{RT},$$

where Y_2 designates the mole fraction of a metal in the vapor phase, f_1 stands for the fugacity of pure water, ϕ_2^∞ is the fugacity coefficients of the dissolved species at its infinite dilution in water, V represents the molar volume of a solid phase, $P^{\otimes}$ =0.1 MPa is the standard pressure.

The values of K^{o} can be calculated from the thermochemical data with the relation

$$-RT\ln K^{o} = g_T(\mathrm{MeO}\cdot(\mathrm{H_2O})_n(g)) - g_T(\mathrm{MeO(s)}) - g_T(\mathrm{H_2O(g)})$$

, where g_T is the Gibbs energy of a compound at the standard pressure. Note that, as a rule, the thermodynamic properties of the hydroxides in the ideal gas state are unknown. The evaluation of the fugacity coefficients of the dissolved hydroxides in the present work is done according to the equation that follows from the virial equation of state [*Prausnitz et al., 1999*]:

$$\ln\phi_2^{\infty} = \frac{2B_{12}}{V_1} - \ln\frac{PV_1}{RT},$$

where B_{12} is the second mixed virial coefficient for the gas-phase interaction between a hydroxide and water, and V_1 stands for the molar volume of pure water. In the current work, the estimation of B_{12} is made using the relation $B_{12} \approx k \cdot B_{11}$, where B_{11} is the second virial coefficient of water [*Harvey and Lemmon, 2004*], and k is assumed to be equal to the number of hydroxide groups and oxygen atoms in the molecule of a dissolved oxide or hydroxide.

As an example, Fig. 1 shows the values of the solubility of quartz in the vapor phase of water for a number of pressures, calculated under the assumption of the existence of a single form $Si(OH)_4(g)$, in comparison with the available experimental data. The required values of the thermodynamic properties of $Si(OH)_4(g)$ are taken from [*Plyasunov, 2011*]. As can be seen, the agreement between the experiment and calculation is quite satisfactory.

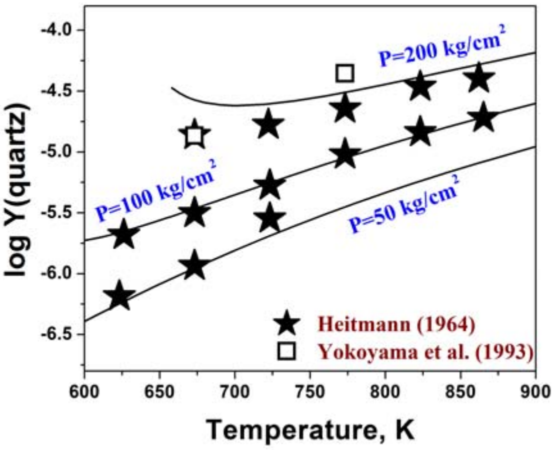

Fig. 1. The experimental and calculated values of the solubility of quartz in the vapor phase of water

At the same time, the calculated solubility of ZnO(s) in steam at 623 K under the assumption of the formation of a single form $Zn(OH)_2(g)$, shown by the dashed line in Fig.2, is an order of magnitude lower than the experimental value at 16 MPa [*Bénézeth et al., 2002*].

One possible reason for discrepancies between the experiment and calculations is that it is necessary to take into account the existence of clusters in the vapor phase, such as $Me(OH)_n\cdot(H_2O)_m$. Thus the task is to calculate by the quantum chemistry methods the thermodynamic properties of such clusters in the ideal gas state over a wide temperature range, and on this basis, to evaluate the relative stability constants of these clusters.

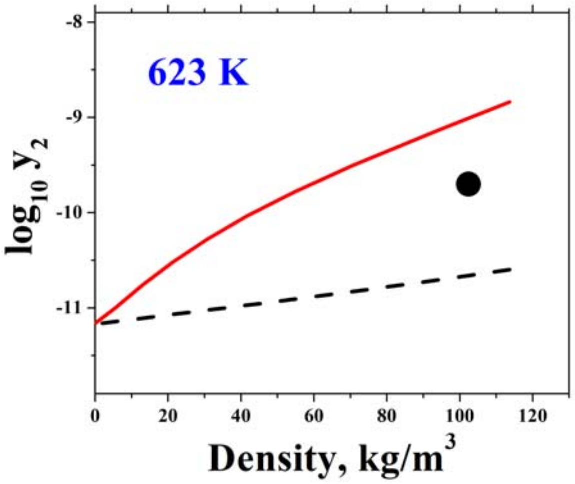

Fig. 2. The calculated values of the solubility of ZnO(s) in the vapor phase of water at 623 K in comparison with the experimental value at 16 MPa [*Bénézeth et al., 2002*]. The dashed line shows the calculated values, obtained under the assumption of the formation of a single form $Zn(OH)_2(g)$, and the solid line corresponds to the calculation with the formation in steam of $Zn(OH)_2(g)$, $Zn(OH)_2{\cdot}H_2O(g)$ и $Zn(OH)_2{\cdot}(H_2O)_2(g)$

Quantum chemical calculations were based on the density functional theory (DFT) with the hybrid functional B3LYP and a set of basic wave functions 6-311G+(d,p) for the "light" atoms (A <79 g mol^{-1}) and using the effective core potential LANL2DZ for A > 79 g mol^{-1}.

The calculations resulted in the thermodynamic description of some compounds $Me(OH)_n{\cdot}(H_2O)_m$ in the ideal gas state over a wide temperature range (273–1273 K).

For the ZnO–H_2O system, such calculations were performed for gaseous clusters of the compositions $Zn(OH)_2$, $Zn(OH)_2{\cdot}H_2O$, $Zn(OH)_2{\cdot}(H_2O)_2$ and $Zn(OH)_2{\cdot}(H_2O)_4$. For the consecutive reactions of hydration of zinc hydroxide in the gas phase, the following values of equilibrium constants at 623 K were obtained:

$$Zn(OH)_2(g) + H_2O(g) = Zn(OH)_2{\cdot}H_2O(g) \qquad \ln K_1 = -3.95$$
$$Zn(OH)_2(g) + 2H_2O(g) = Zn(OH)_2{\cdot}(H_2O)_2(g) \qquad \ln K_2 = -7.92$$
$$Zn(OH)_2(g) + 4H_2O(g) = Zn(OH)_2{\cdot}(H_2O)_4(g) \qquad \ln K_4 = -23.91$$

The distribution of zinc forms depending on the density of steam at 623 K is shown in Fig. 3, left.

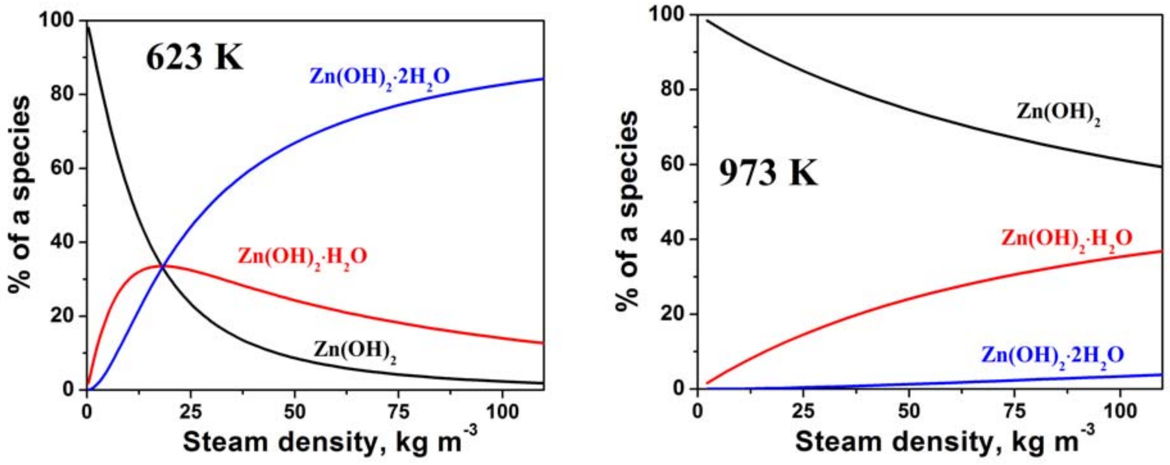

Fig. 3. The distribution of zinc forms in steam at 623 K (left) and 973 K (right) depending on the water density

Clearly, at 623 K the unhydrated hydroxide predominates only at very low densities of steam ρ_1, at intermediate values of ρ_1 the fraction of monohydrate $Zn(OH)_2{\cdot}H_2O$ is appreciable, and at the water densities above 25 kg m^{-3} dihydrate $Zn(OH)_2{\cdot}(H_2O)_2$ dominates absolutely. The contribution of tetrahydrate is negligible at these conditions. The consideration of all forms significantly increases the calculated solubility of ZnO(s) in steam at 623 K (see the solid line in Fig. 2).

According to calculations, the distribution of zinc forms in steam depends strongly on the temperature, and the dehydration of the species with the increasing temperature is obvious. For example, with the increase of the temperature to 973 K the predominant form of zinc becomes the unhydrated hydroxide, over the entire range of considered vapor densities, 0–100 kg m^{-3} (Fig. 3, right).

Conclusions

The analysis of transport processes of compounds in the gas phase requires the knowledge of the stoichiometry of forms and their thermodynamic properties.

The methods of quantum chemistry allow calculating thermochemical properties of various forms of the type $Me(OH)_n{\cdot}(H_2O)_m$ in the ideal gas state and evaluating their relative stability.

The application of these methods to the Me-O-H systems showed that in the gas phase not only hydroxides are stable, but also hydrates of hydroxides, and in many cases, the contribution of hydrates is predominant.

The consideration of all forms of metals greatly increases the calculated solubility of the compounds in the vapor phase, often improving the agreement between the experimental and calculated values.

This work was supported by the grants of RFBR 11-05-00786-a and 12-05-93107-CNRSL_a .

References:

1. Bénézeth, P., D.A. Palmer, D.J. Wesolowski, C. Xiao (2002). New measurements of the solubility of zinc oxide from 150 to 350°C, *J. Solut. Chem.*, 31, 947–973.

2. Harvey, A. H., E. W. Lemmon (2004). Correlation for the second virial coefficient of water, *J. Phys. Chem. Ref. Data*, 33, 369–376.
3. Heitmann, H. G. (1964). Solubility of silicic acid in water and steam and its effect on silica deposits in turbines (in German), *Chemiker-Zeitung*, 88, 891–893.
4. Plyasunov, A.V. (2011). Thermodynamic properties of H_4SiO_4 in the ideal gas state as evaluated from experimental data, *Geochim. Cosmochim. Acta*, 75, 3853–3865.
5. Prausnitz, J. M., R. N. Lichtenthaler, E. G. de Avezedo (1999). Molecular Thermodynamics of Fluid-Phase Equilibria, *3rd Edition, Prentice-Hall*, New York, 860 p.
6. Yokoyama, C., A. Iwabuchi, S. Takahashi, K. Takeuchi (1993). Solubility of PbO in supercritical water, *Fluid Phase Equil.*, 82, 323–331.

Bublikova T. M., Setkova T. V., Balitsky V. S.

Study of heat-mass transfer mechanisms and estimation of mass flow of vapor in recirculated crystallizers

Institute of experimental mineralogy RAS, Chernogolovka
tmb@iem.ac.ru

The construction of crystallizer of recirculated type with the prospect of growth in it malachite, azurite and other compounds was developed based on experimental and theoretical data on heat and mass.

Key words: recirculated crystallizers, heat-mass transfer, synthesis of minerals

Reference: Bublikova, T.M., T.V. Setkova, V.S. Balitsky (2012), Study of heat-mass transfer mechanisms and estimation of mass flow of vapor in recirculated crystallizers, *Vestnik ONZ RAS, 4,*

The investigations of heat-mass transfer mechanisms in closed type crystallizer (original construction of IEM RAS) as part of study on the synthesis of dense aggregates of malachite (basic copper carbonate) [*Balitsky et al, 1987; Bublikova et al, 2000; Balitsky et al, 2009*] were carried out. The crystallizers of this type are used to grow crystals which characterized by the inverse temperature coefficient of solubility (TCS). The most suitable for the synthesis of malachite in a closed system is crystallizer in which the volatile solvent makes repeated recycling through phases: liquid → vapor → liquid (dissolution of the charge) → liquid (crystallization of malachite) → vapor and so on.

To estimate the characteristic parameters and understanding the processes of heat-mass transfer (HMT), was made theoretical calculations and was determined mass flow of vapor in the process of modeling a procedure of malachite synthesis in pure water at temperatures up to 100°C experimentally.

Heat removal from the condenser was realized by the flow of running water, heat input to the crystallization zone – an electric heater. In the steady state the process is characterized by temperature constant at different points on height of apparatus and the constancy of the circulation of water in the thermal loop. Heat transfer inside the apparatus account for several processes, therefore was estimated a quantitative contribution of each of them. Heat transfer between the upper hot (80°C) and lower cold (20°C) zones inside the crystallizer is affected by: a) free convection gas-vapor mixture, b) condensation of convecting vapor from a mixture, c) radiant radiation. Simplified calculations [*Kutateladze, 1958*] of heat-mass transfer parameters showed that the main contribution to heat transport makes condensation of convecting vapor: $\alpha_{cond.} = 4.8 \bullet 10^{-3}$ kcal/m sec.°C, $\alpha_{conv.} = 8.4 \bullet 10^{-4}$ kcal/m sec.°C, $\alpha_{rad.} = 15–20\%\ \alpha_{cond} + \alpha_{conv}$. Calculated value of mass vapor flow (m_n) is $0.54\ 10^{-3}$ kg/m^{2}sec.

The experimental determination of mass vapor flow in the crystallizer at the same temperature and pressure simultaneously with the calculations was carried out. Experiments were performed in a laboratory crystallizer with volume of $6.8\ 10^{-3}$m^3 (fig. 1). Crystallizer is a built-up structure consisting of two chambers of square cross section and tightly connected by a flange connection. In the upper cover of crystallizer is mounted a water condenser. The crystallizer is divided horizontal partition at a height h = 80 mm from the bottom, which has a central opening square cross section for the vapor to escape. The partition served as a sampler. The crystallizer was filled water to the level of 0.02 m, sealed and placed in an electric furnace. Bottom temperature was maintained constant of 80 ± 1°C, the temperature of the upper cover was equal to 20 ± 1°C. As a result of a continuous process of water evaporation in the hot zone and vapor condensation on the cooler the part of condensate was got to the sampler. At specified time the condensate was poured and measured its volume. Duration run was 15, 30, 45, 60 minutes. The area of sampler was equal to 0.02 m^2. The experimental results are shown in table 1. They are in satisfactory agreement with the calculated data.

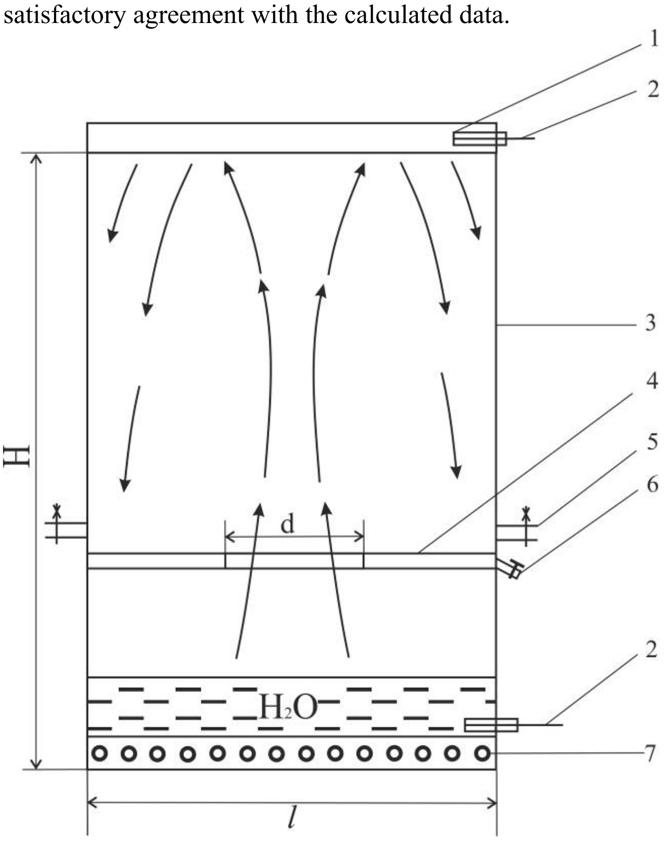

Fig. 1. The sketch of laboratory crystallizer for experiments to determine of mass vapor flow: 1 – condenser, 2 – thermocouples, 3 – crystallizer body, 4 – sampler, 5 – flanges, 6 – bibcock, 7 – electrical heater

Table 1. The conditions and results of experiments to determine of mass vapor flow (m_n)

No	Run time, min.	T hot zone, °C	T cold zone, °C	Water volume in sampler, ml	Mass vapor flow m_n exp., kg/m^2c
1	15	80	20	27	$1.5\cdot10^{-3}$
2	15	80	20	24	$1.33\cdot10^{-3}$
3	15	81	20	30	$1.67\cdot10^{-3}$
4	30	80	20.5	47	$1.31\cdot10^{-3}$
5	30	80	20	51	$1.42\cdot10^{-3}$
6	30	80	20	48	$1.33\cdot10^{-3}$
7	45	80	20	75	$1.39\cdot10^{-3}$
8	45	80	20	75	$1.39\cdot10^{-3}$
9	45	80	19.5	77	$1.43\cdot10^{-3}$
10	60	81	20	108	$1.5\cdot10^{-3}$
11	60	81	20.5	105	$1.46\cdot10^{-3}$
12	60	80	20	99	$1.38\cdot10^{-3}$

A similar approach to estimate of influence of height placement of charge basket and diameter of central hole through which the vapor transferred on parameters of heat-mass transfer was used. Figure 2 illustrates the scheme of the process. In contrast to apparatus considered on fig. 1, in this crystallizer was set basket with charge $Cu_2(OH)_2CO_3$, aqueous ammonia solution was used as solvent. The size of hole in basket influences on process. If hole narrowed then free-convective heat transfer decreased and, as consequently decreased the intensity of the condensate supply to charge up to almost complete stop of the process.

The placement of charge basket over the crystallizer bottom (h) influence of process dynamics. We can purposefully set temperature of seeping through the charge solution and consequently concentration of dissolved components, if we change coordinate of the vertical placement of charge basket (h).

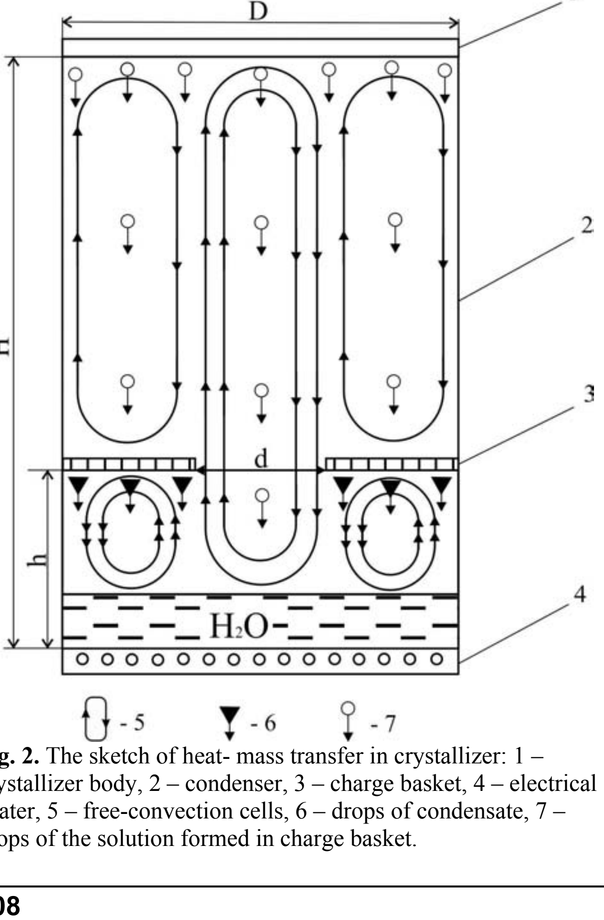

Fig. 2. The sketch of heat- mass transfer in crystallizer: 1 – crystallizer body, 2 – condenser, 3 – charge basket, 4 – electrical heater, 5 – free-convection cells, 6 – drops of condensate, 7 – drops of the solution formed in charge basket.

The height of the basket in crystallizer is determined by two conflicting requirements. The temperature in the basket must be low enough so that the excess salt concentration in the solution entering the hot zone compared with the equilibrium concentration was sufficient for keeping of maximum rate of crystal growth of minerals (it is provided by temperature gradient 25–45°C between bottom and charge basket). On the other hand, this temperature must be above some critical value at which the super saturation is achieved at entering solution in crystallizer bottom and leading to anomalous high growth rates (homogeneous nucleation and mass crystallization, etc.). Based on calculations and experiments the optimal height of placement of charge basket corresponds to the values h/H=0.25–0.8.

The construction of crystallizer of recirculated type with the prospect of growth in it malachite, azurite and other compounds was developed based on experimental and theoretical data on heat and mass.

References:

1. Balitsky, V. S., T. M. Bublikova, S. L. Sorokina, L. V. Balitskaya, A. S. Shteinberg (1987). Synthetic jewelry semi-precious malachite, *Doklady Akademii Nauk SSSR*, 297, pp. 184–186.
2. Balitsky, V. S., T. M. Bublikova, Yu. B. Shapovalov (2009). Synthetic ornamental malachite - a perspective facing material for building and construction industry*, Journal of BGTU V.G. Shukhov*, 3, pp. 4–11.
3. Bublikova, T. M., V. S. Balitsky, I. V. Timokhina (2000). Synthesis and basic properties of the jewelry and ornamental malachite, *Synthesis of mineral*, Alexandrov VNIISIMS, pp. 502–532.
4. Kutateladze, S.S., V.M. Borishansky (1958). *Handbook of heat transfer*, Moscow. p. 414

Vasina[1] O.N., Shikina[2] N.D., Gurova[1] E.V., Popova[1] E. S., Tagirov[2] B. R., Khodakovsky[1,3] I. L. Thermodynamic properties of zirconium hydroxo-complexes in aqueous solutions

[1] Dubna International University of Nature, Society, and Man, Dubna

[2] Institute of Ore Deposite Geology, Petrography, Mineralogy and Geochemistry RAS, Moscow

[3]V. I. Vernadsky Institute of Geochemistry and Analytical Chemistry RAS, Moscow medolik@list.ru

Experimental data on solubility of ZrO_2 in aqueous solutions of chloric acid at 150 and 250°C, the equations of the temperature dependences of equilibrium constants of dissolution reactions of ZrO_2 and thermodynamic properties of zirconium hydroxo-complexes and ion Zr^{4+} (aq) at 25°C are presented.

Key words: zirconium dioxide, solubility, aqueous solutions, hydroxo-complexes, a zirconium ion, thermodynamic properties.

Citation: Vasina, O. N, N. D. Shikina, E. V. Gurova, E. S. Popova, B. R. Tagirov, I. L. Khodakovsky (2012), Thermodynamic properties гидроксокомплексов zirconium in water solutions, *Vestn. Otd. nauk Zemle, 4,*

Getsina M. L., Toropchenova E. S., Nabiullina S. N., Koshcheeva I.Ya., Kubrakova I.V. Simulation of migration colloidal gold in surface waters of natural

V.I. Vernadsky Institute of Geochemistry and Analytical Chemistry RAS, Moscow kubrakova@geokhi.ru

With the purpose of studying migration and accumulation nature of the colloidal metal forms in natural and anthropogenic environments the conditions for nanoscale metal forms, stabilized by low molecular and macromolecule organic ligands with the example of gold were defined. The kinetics and completeness of obtained particle concentrating with goethite (FeOOH) in circum neutral environments were studied. It is established, that gold particles stabilized with natural ligands of humus nature, interact with goethite most quickly, providing both efficient colloid transport of gold and its deposition on geochemical barriers.

Key words: nanoscale gold, preparation, sorption by goethite

Ref: Getsina, M. L., E. S. Toropchenova, S. N. Nabiullina, I. Ya. Koshcheeva, I. V. Kubrakova (2012), Simulation of migration colloidal gold in surface waters of natural, *Вестник ОНЗ РАН, 4,* (doi:)

Nanoscale metal forms, including gold, are very common in natural systems and are an intermediate link in the mineralization processes. Depending on the conditions the superfine particles can either be dissipated by migrating as a fluid component (as dissolved compound forms, stabilized colloids or pseudocolloids), or concentrating on geochemical barriers up to ore deposits formation. The paper considers the possibility of nanoscale gold forms preparation, stabilized by natural organic substances, and their deposition kinetics in the circum neutral environments on goethite (FeOOH) – one of the main components of natural suspensions and bottom sediments.

As an example of nanoscale gold forms stabilized low molecular organic compounds, particles in the size range of 10–20 nm prepared during the $HAuCl_4$ reduction in the presence sodium citrate [*Turkevich, 1953*] were considered. Monodisperse gold nanoparticles stabilized citrate, have been obtained by the microwave hydrothermal synthesis and characterized by the plasmon resonance spectra, as well as the scanning electron microscopy (SEM). The effect of preparation conditions (pH, temperature, time, reagent ratios) on the size, shape and amount of produced particles. It is established, that the most stable monodisperse gold nanoparticles (10–20 nm) produced in the pH range of 5.0–6.0 at 100–130 °C. The maximum plasmon resonance wavelength and the intensity of absorption are practically identical and correspond to the wavelength of 522–524 nm. The study of the colloidal gold formation kinetics at pH of 5.5 and 100 °C showed that the particles take the final size and shape during the first minutes of synthesis with the molar ratio of reagents of 1:1.

Nanoscale gold forms, stabilized macromolecule organic substances of humus nature – fulvic acids (FA), allocated from the natural color of water by the method [*Varshal, 1973*] obtained and investigated the same way. FA concentration for the synthesis was 120 µg/ml. Fig. 1 shows the plasmon resonance spectra of colloidal gold, stabilized sodium citrate (curve 1) and FA (curve 2), as well as the electronic absorption spectrum of the dissolved gold (curve 3). Electronic microphotography of colloidal gold particles, stabilized FA and received in the chosen conditions, is shown in Fig. 2.

The behavior of nano-sized gold, stabilized organic matter of a different nature, at interaction with the suspended (sedimentary) matter, studied in the model sorption experiments with the use of synthetic amorphous iron oxyhydroxide as sorption phase. The kinetics of the gold particles sorption studied in the pH range of 5.0–7.0, which is typical for surface waters, in comparison with the kinetics of the dissolved inorganic forms sorption [*Kubrakova, 2011*]. Concentration of gold in the solutions over the residue was determined by ETAAS.

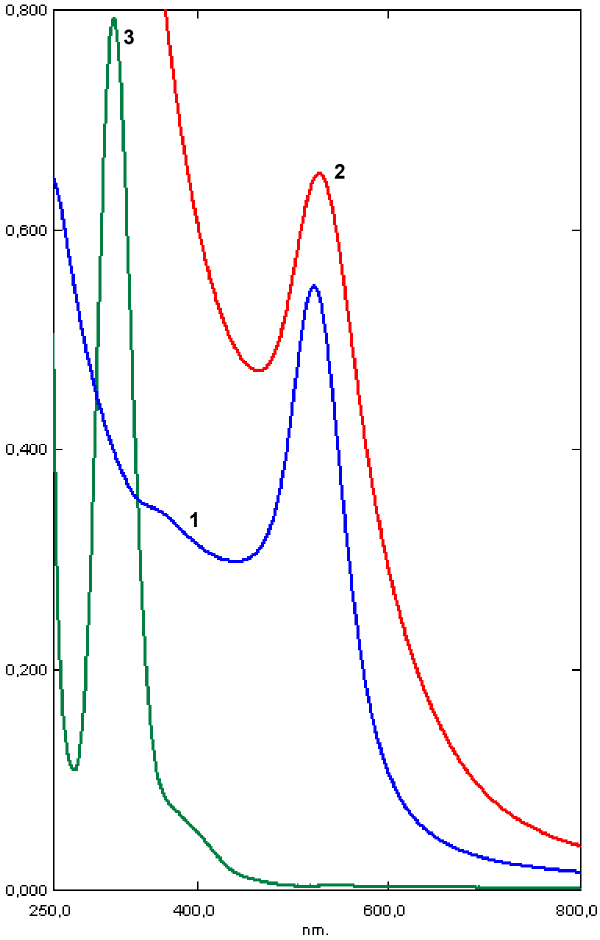

Fig. 1. Plasmon resonance spectra of colloidal and dissolved gold: particles, stabilized sodium citrate (1); particles, stabilized FA (2); hydrogen tetra-chloroaurate solution (3)

Fig. 3 shows the sorption of colloidal gold, stabilized FA (1), gold sols, stabilized citrate (2), and dissolved inorganic gold (III) forms (3) at pH6.0. It seems that at the interaction of nano-sized Au^{o}, stabilized FA, with iron oxyhydroxide sorption equilibrium is achieved most quickly – in several hours. This is caused, probably, the strength of covalent binding of polyfunctional natural ligand, stabilizing nanoscale metal particle, with the surface of the iron oxyhydroxide by the complexation mechanism. In the case of inorganic gold complex, as well as colloidal gold, stabilized low-molecular citrate ions, sorption equilibrium is established in several days.

Thus, goethite interacts with both the molecular and with nanoscale gold forms, providing their migration and accumulation in aquatic environments regardless of the metal form. At the same time, organic matter, especially humus nature, substantially (dozens of times) accelerates the interaction of gold with iron oxyhydroxide, providing both colloid transport of gold and its deposition on geochemical barriers. This fact allows to consider nanoparticles, stabilized humic substances, as the most active migration form of gold in natural waters.

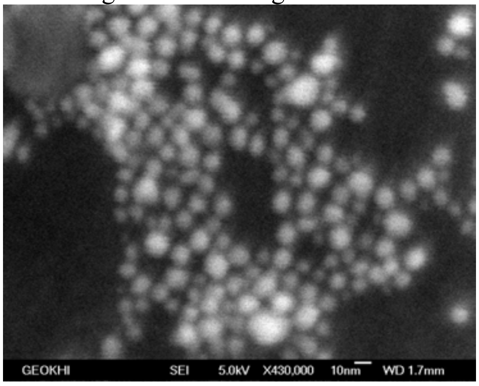

Fig. 2. SEM image of gold nanoparticles, stabilized FA (Jeol JSM 6700F, the scanning area 245x180 nm)

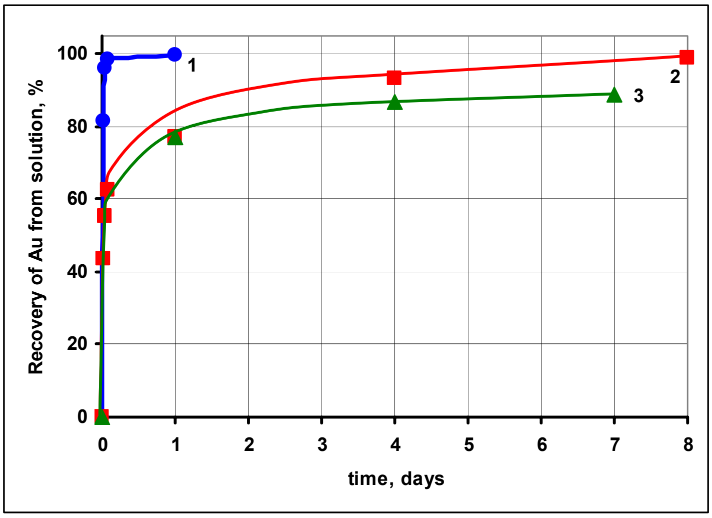

Fig. 3. Sorption of Au°, stabilized FA (1), Au°, stabilized sodium citrate (2) and inorganic Au(III) complex (3) by goethite as a function of time at pH6.0

References:

1. Kubrakova, I. V., A. V. Fortygin, S. G. Lobov, I. Ya. Koshcheeva, O. A. Tyutyunnik, M. V. Mironenko (2011). Migration of platinum, palladium, and gold in the water systems of platinum deposits, *Geochem. Int.*, Vol. 49, №11, p. 10721084.
2. Turkevich, J., P. C. Stevenson, J. Hillier (1953). The formation of colloidal gold, *J. Phys. Chem.*, 57, p. 670.
3. Varshal, G. M., T. K. Velyukhanova, I. S. Sirotkina (1973). Fractionation, Quantitative Determination, and Study of Some Major Components of Dissolved Organic Matters of Natural Waters, *Gidrokhim. Mater.* 59, p. 143–151.

Zaitsev V. A., Gruzdeva A. A., Starshinova N. P., Khamizov R. Kh., Kogarko L. N. On the gel of silica formed by the acid decomposition of eudialite concentrate

V. I. Vernadsky Institute of Geochemistry and Analytical Chemistry RAS, Moscow alkaline@geokhi.ru

We studied silica-rich gel, formed by the acid decomposition of eudialine and nepheline. The gel shows week sorption selectivity of rare metals. Gels of silica are formed in various geological processes, including ultroagpaite rocks and pegmatites as intermediate compounds and can be fixed due to formation of opal, sometime containing significant concentrations of admixture elements. It can be supposed: if the gel of silica is formed in the way of migration of low-temperature solutions, the selective sorption of metals can be effective mechanism of local differentiation of components.

Key words: experiment, acid decomposition of eudialite,gel-type silica, sorption

Reference: Zaitsev, V. A., A. A. Gruzdeva, N. P. Starshinova, R. Kh. Khamizov, L. N. Kogarko (2012), On the gel of silica formed by the acid decomposition of eudialite concentrate, *Vestnik ONZ RAS, 4*,

Acid leaching is one of the key stage of any technology for recovery rare-element from eudialite. We experimentally studied eudialite decomposition by HCl and HNO_3 to search the optimal parameters of obtaining the solutions of rare- and rare-earth elements for their further separation.

The sample of eudialite concentrate, provided by the Lovosersky GOK, was used as a starting material. The concentrate contained eudialite (71.1 %), aegirine+arfvedsonite (12.3%), nepheline(8.9%), feldspar (2.4%), loparite (0.4%), lamprpophyllite and lorenzenite (4.41%). During the experiment, the sample of concentrate was treated by the acids for 1–3 days.

X-ray diffraction spectra show reflexes of aegegine, arfvedsonite, feldspar and loparite, but do not show presence of nepheline and eudialite. Nepheline and eudialite are decomposed with formation of gel, which can be filtrated through a red-dot filter, but do not penetrate through the white-dot filter. Mass-balance calculations show, that water content in the gel strongly depends on the concentration of used acid: the weak acid (3%) forms gel, containing 90% of water, whereas the gel, formed by the 30% acid contains only 75% of water. The gel also contains rare and rare-earth elements, and this determines the importance of the elaboration of eudialite technology.

At study of properties of the gel, the filter cake was washed by distilled water with the use of step-by-step technique. Composition of liquids was determined by ICP-MS and ICP-AS methods (GEOKHI RAS).

Concentration of metals in wash liquid (C) can be approximated by exponential function $C = C_o*B*exp(A*V)$, where V is the volume of filtered solution and C_o is the concentration of element in initial material (before experiment). A and B are empirical coefficients.

We found that metal/metal ratios are gradually change from earliest portions of water to the lasts: for example, Ce/La increases from 2.56–2.66, to 2.77–5.23, Y/La ratios in the earliest solutions are 2.11–2.19, but in the latest one it goes up to 2.71. Zr/Y ratio changes from 14–18.3 to 16–41. It is interesting, that the gel mostly selective on Zr/Y do not show selectivity to REE. Zr/Ti values decrease from 11.2–13.1 to 5–7, sometime, the intermediate stage show the lowest ratio: 2.2–3.5. We suppose that it is the evidence of sorption selectivity which strongly vary from experiment to experiment.

Gels of silica are formed in various geological processes as intermediate compounds and can be fixed due to opal formation in various geological setting, including ultroagpaite rocks and pegmatites. For example, opals, containing significant concentrations of Na, Al, and Zr were found in Lovosero massif [*Pekov, 2000*], opals with Na, Cl, Ca, Zn, Hg – in Yellowstone hot springs field [*Channing, 2007*].

It can be supposed: if the gel of silica is formed in the way of migration of low-temperature solutions, the selective sorption of metals can be effective mechanism of local differentiation of components.

This work was supported by Russian Foundation for Basic Research.

References:

1. Pekov, I. V. (2000). Lovosero Massif: History. Pegmatites. Minerals, Ocean Pictures Ltd, Russia, 484 pp.
2. Channing, A., I. B. Butler (2007). Cryogenic opal-A deposition from Yellowstone hot springs, Earth and Planetary Science Letters, vol. 257, iss. 1–2, pp. 121–131.

Zotov[1] A. V., Akinfiev[1] N. N., Volchenkova[2] V. A., Selivanov[3] P. V. Chlorargyrite (AgCl) solubility in low density hydrothermal fluids

[1]Institute of Geology of Ore Deposits, Petrography, Mineralogy and Geochemistry RAS, Moscow
[2]*Institute of Metallurgy and Material Science* RAS, Moscow
azotov@igem.ru
[3]Russian State Geological Prospecting University, Moscow

The goal of the study is to experimentally verify available experimental data and to modify equation of state proposed recently by *Akinfiev and Diamond* [*2003*] for thermodynamic description of neutral aqueous species in a wide range of thermal solvent densities expanding a low density region (ρ = 0.05–0.3 g·cm^{-3}). Solubility of chlorargyrite AgCl(s) was measured in aqueous solution at 400 °C vs. pressure (P = 100–400 bars), i.e. for the fluid densities from 0.04 to 0.5 g·cm^{-3}. Our previous data on the AgCl(s) solubility [*Voronin et al., 2005*] in a low density region of H_2O may be overestimated because of a methodological shortcoming (pressure was not under control during the experiment).

Key words: experiment, solubility of AgCl, low density fluid, equation of state

Reference: Zotov, A. V., N. N. Akinfiev, V. A. Volchenkova, P. V. Selivanov (2012), Chlorargyrite (AgCl) solubility in low density hydrothermal fluids, *Vestnik ONZ RAS, 4* (*doi:*)

Experimental technique

Experiments were carried out at 400 ± 1 °C in titanium alloy VT 8 autoclaves with the internal sampler [*Zakirov, Sretenskya, 1994*]. The pressure was measured by strain-gauge sensor D100 calibrated by the deadweight pressure system MP-2500 with an error less than 1%. Chemically pure (CP) AgCl pressed into tablets under a pressure of 30 kg·cm^{-2} was used as a solid phase reagent. The volume of titanium sampling ampoules was of 6.5 cm^3, the rest volume of the autoclave was 94 cm^3.

The experimental cycle was as following. At the bottom of autoclave the specified amount of distilled water was poured to produce required pressure at given temperature. In the medium part of the autoclave a titanium pan with 5–6 pieces of AgCl(s) (of 0.5–0.8 g) was located. The titanium sampling ampoule was located in the hood of the autoclave and was locked by a valve needle through Pt gasket. Graflex was used to seal the rod of the valve in the autoclave. The ampoule preliminary thoroughly washed by chloronitric acid was initially closed. After heating and 2–3 days staying at 400 °C ampoule has been opened for a few minutes. Herewith pressure lowered by ca 3–5 %. Then ampoule was closed again, the autoclave was removed from the oven and quenched in cold water while its top was aired by a fan.

Subsequently the ampoule was 2 times washed by a triple diluted hot aqua regia. The wash-outs were analyzed separately after addition of amount of water to get 4–5 times dilution of the aqua regia. Silver in the solution was determined by atomic emission spectrometer with inductively coupled plasma (ICP spectrometer by "JOBIN YVON HORIBA", France, the model "ULTIMA-2"). The detection limit of silver was 0.5 ppb. The content of silver in the blank samples was about 1 ppb. The content of silver in the 2nd washout was usually an order of magnitude smaller than in the 1st. In addition Ag-bearing solution of the autoclave without washing its walls was also analyzed. The concentration of Ag in these samples was typically an order of magnitude lower than the concentration in the fluid from the ampoule, probably due to precipitation of silver chloride on the walls of the autoclave during quenching. In dense fluids where AgCl (s) solubility is high the concentration of silver was determined by the weight loss method.

Experimental results

The experimental conditions and measured values of AgCl(s) solubilities are given in Table 1.

It's found out that in relatively dense fluids (0.3–0.5 g·cm^{-3}) solubility of chlorargyrite slightly increases with increasing pressure, whereas in low-density ones with decreasing pressure and the corresponding density from 0.3 to 0.05 g·cm^{-3} solubility shows sharp fall of about 3 orders of magnitude. In the coordinates of lg m_{Ag} – lg P_{H_2O} the dependence of the AgCl(s) solubility is expressed a straight line with a slope of about 7.5.

Table 1. Solubility of AgCl(s) in water at 400 ± 1 °C as a function of pressure

P, bar	ρ, g·cm^{-3}	m(Ag), mol·(kg H_2O)$^{-1}$	
		ICP	weight loss
108	0.0413	-5.89	
142	0.0592	-5.69	
152	0.0651	-5.35	
198	0.0996	-4.87	
246	0.1615	-3.96	
265	0.2036	-3.61	
284	0.2964		-2.78
296	0.3542	-3.00	-2.81
335	0.4558	-2.62	-2.7
357	0.4780	-2.55	
380	0.5073		-2.59
400	0.5240		-2.47

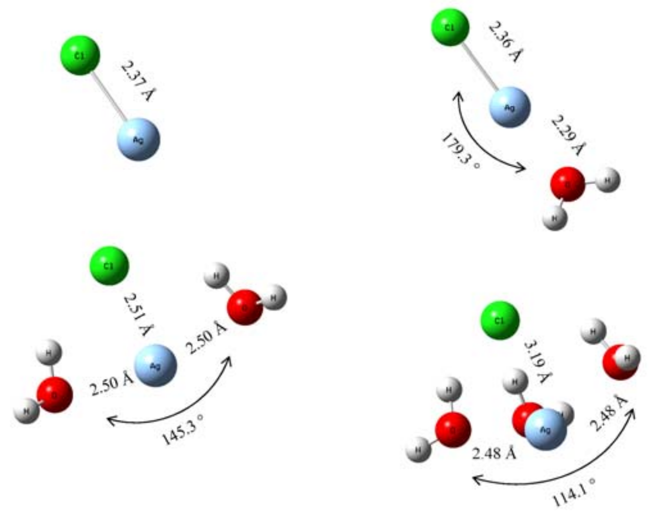

Evaluation of experimental data

Initially to identify the stoichiometry of silver species in hydrothermal low-density fluid the thermochemical properties of AgCl, $AgCl(H_2O)$, $AgCl(H_2O)_2$, $AgCl(H_2O)_3$ molecules in the state of perfect gas for temperature range 298–1000 K by means of quantum chemistry (DFT B3LYP, Cl, O, H – 6-311+G(d,p), Ag – core potential LANL2DZ) were evaluated. The optimized structures are shown in Figure 1.

Fig. 1. Optimized by means of quantum chemistry computations structures of H_2O clathrates of AgCl ion pair in the state of a perfect gas. Numbers stand for bond distances in Å and angles in degrees

The thermochemical data obtained enable to compute equilibrium constants of the gaseous Ag-bearing species in the reaction of the type

$$AgCl + nH_2O = AgCl(H_2O)_n$$

In this case equilibrium constant of the reaction should be expressed in the form:

$$\ln K_a = -\frac{\Delta_r G_T^o}{RT} = \ln\frac{f_{AgCl(H_2O)_n}}{f_{AgCl}\cdot f^n_{H_2O}} = \ln\frac{p_{AgCl(H_2O)_n}\cdot\gamma_{AgCl(H_2O)_n}}{p_{AgCl}\cdot\gamma_{AgCl}} - n\cdot\ln f_{H_2O}$$

Assuming that fugacity coefficients of different Ag bearing species in the H_2O fluid are close to each other get the relation for ratio of their molalities in the fluid can be obtained

$$\ln\frac{p_{AgCl(H_2O)_n}\cdot\gamma_{AgCl(H_2O)_n}}{p_{AgCl}\cdot\gamma_{AgCl}} \approx \ln\frac{p_{AgCl(H_2O)_n}}{p_{AgCl}} = \ln\frac{m_{AgCl(H_2O)_n}}{m_{AgCl}} = \ln K_a + n\ln f_{H_2O}$$

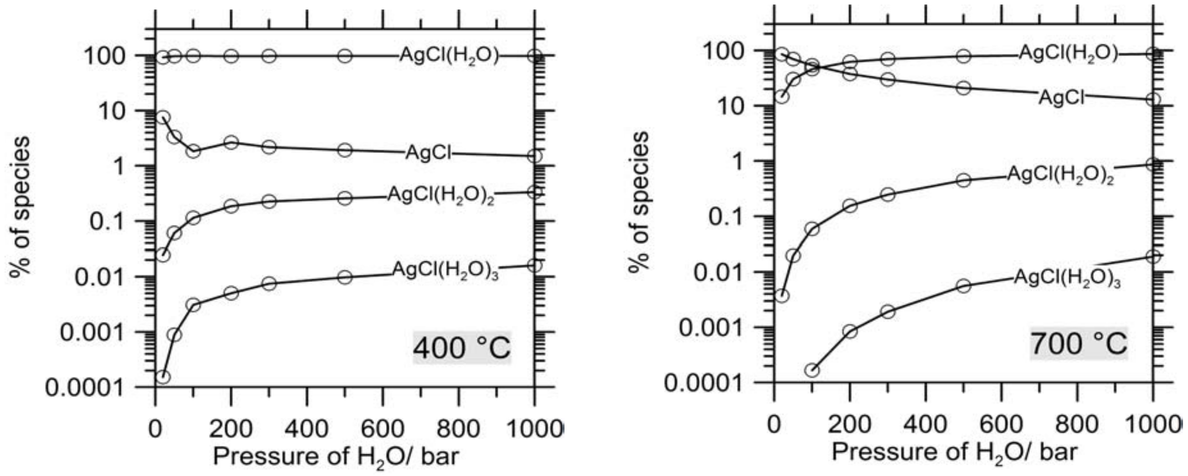

Fig. 2. Computed distribution of various Ag-bearing species (in mol %) in aqueous fluid as a function of H_2O pressure at 400 ºC (left) and 700 ºC (right)

The calculation results shown in Fig. 2 indicate that the linear associate, $AgCl(H_2O)$ (sp-hybridization of Ag), is prevalent in the whole temperature range 0 - 600 ºC. Only at temperatures > 700 ºC and vapour pressures < 100 bar the anhydrous AgCl becomes a prevalent form.

The equation of state (EoS) (Akinfiev, Diamond, 2003) was employed to describe the experiment data. Because the prevailing form of Ag species has a high dipole moment the additional term, namely $\omega\left(\frac{1}{\varepsilon}-1\right)\cdot 10^5$, was introduced into the EoS. Here ω, the Born parameter [*Tanger, Helgeson, 1988*], reflects

According to the computations concentrations of $AgCl(H_2O)_2$ and *a fortiori* $AgCl(H_2O)_3$ are void for the entire range of temperatures and pressures. Therefore, further fit of model parameters has been carried out solely for the monohydrate, AgCl (H_2O).

electrostatic interactions of the Ag species with the surrounding water molecules:

$$\mu^o_{aq}(P,T) = \omega\left(\frac{1}{\varepsilon}-1\right)\cdot 10^5 + \mu^o_g(T) - RT\ln N_w + (1-\xi)RT\ln f_1^o + $$
$$+ RT\xi\ln\left(\frac{\tilde{R}T}{M_w}\rho_1^o\right) + RT\rho_1^o\left[a + b\left(\frac{10^3}{T}\right)^{0.5}\right].$$

Thus, the basis of the resultant description are quantum-chemical calculations of $\mu_g^{\circ}(T)$ for gaseous hydrate water associates at standard pressure (1 bar) and the experimental data on chlorargyrite solubility: a) in a dense fluid at 25–300 °C and saturation water pressure [*Zotov et al., 1995*], and b) at 400 °C as a function of H_2O pressure (present study). As a result following values for standard state thermodynamic functions for gaseous hydrate $AgCl(H_2O)$ $\mu^{o}_{298,g}$ = -50300 $cal \cdot mol^{-1}$, $S°_{g,\ 298}$ = 77.281 $cal \cdot mol^{-1} \cdot K^{-1}$, $C°_{p,g}\ (T) = 18.588 + 2.996 \cdot 10^{-3} \cdot T - 0.95 \cdot 10^{5} \cdot T^{-2}$ as well as empirical parameters of the EoS: ξ= -0.38, a = 8.7015, b = -7.3785, ω = 0.143 $cal \cdot mol^{-1}$ were estimated.

Finally, the proposed EoS provides correct AgCl(s) solubility behaviour both vs pressure for supercritical aqueous fluid at 400 °C (solid line in Fig. 3) and vs temperature at 25 – 300 °C in dense fluid at the saturation pressure of H_2O [*Zotov et al., 1995*].

Conclusion

To describe the solubility of AgCl (s) over a wide range of temperatures and pressures, which includes the low-density region of aqueous fluids, the equation of state [Akinfiev, Diamond, 2003] has been modified. This modification provides correct solubility description both at supercritical conditions (400 ° C, 100–500 bar), and the corresponding experimental data at 25–300°C in dense fluid at the saturation pressure of H_2O. The available experimental data of Migdisov et al. [1999] for water vapour at 300–360 ° C are in worse accordance. In order to match the experimental data as well as adjust the parameters of the EoS some additional experiments to determine the solubility of chlorargyrite in subcritical water vapour are desirable.

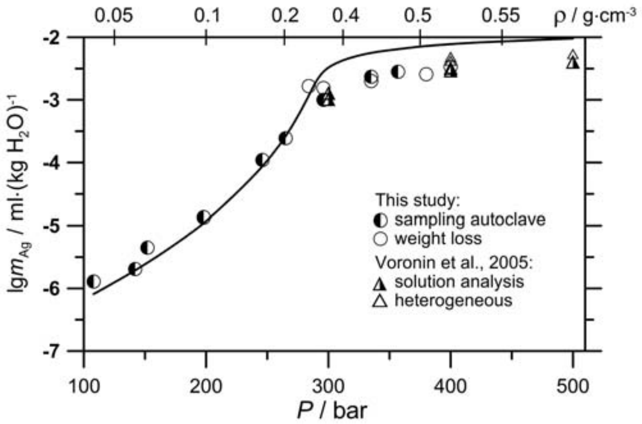

Fig. 3. Comparison of the experimental AgCl(s) solubility with calculated one as a function of H_2O vapour pressure at 400 ºC. Points stand for experiment, line depicts– calculated values after the model adopted in this study

This work was supported by the grant of RFBR 12-05-93107-CNRSL_a.

References:

1. Akinfiev, N.N., L.W. Diamond (2003). Thermodynamic description of aqueous nonelectrolytes at infinite dilution over a wide range of state parameters, *Geochim. Cosmochim. Acta*, 67, 613–627.
2. Migdisov, Art. A., A.E. Williams-Jones, O.M. Suleimenov (1999). Solubility of chlorargyrite (AgCl) in water vapor at elevated temperatures and pressures, *Geochim. Cosmochim. Acta*, 61, 3817–3827.
3. Tanger, IV J.C., H.C. Helgeson (1988). Calculation of the thermodynamic and transport properties of aqueous species at high pressures and temperatures: Revised equations of state for standard partial molal properties of ions and electrolytes, *Amer. J. Sci.*, 288, 19–98.
4. Zotov, A.V., A.V. Kudrin, K.A. Levin, N.D. Shikina, L.N. Var'yash (1995). Experimental studies of the solubility and complexing of selected ore elements (Au, Ag, Cu, Mo, As, Sb, Hg) in aqueous solutions, *In.: Fluids in the Crust. / Shmulovoch K.,Yardley B. and Gonchar G. (eds), Chapman and Hall*, 95–138.
5. Voronin, M.V., N.N. Akinfiev, A.V. Zotov (2005). Solubility of chlorargyrite $AgCl_{cr.}$ in low density aqueous fluid at 400–425 °C and 50–1000 bar, *Geochim. Cosmochim. Acta*, 69 (108), Suppl., p. A735.
6. Zakirov, I.V., N.G. Sretenskaya (1994). Methodology of experimental determination of phases' composition in heterogeneous conditions, *Experimental problems of geology*. M., «Nauka», 664–667.

Kolonin G.R., Shironosova G.P. REE distribution coefficients in monazite–apatite–fluorite association depending on HF and T–P–X parameters of fluids (thermodynamic modeling)

Sobolev Institute of Geology and Mineralogy of the Siberian Branch of the RAS, Novosibirsk shiron@igm.nsc.ru

The dependence of the composition of equilibrium mineral association was shown in the range of 500-100°C. The Ln and Y distribution coefficients between the ideal solid solutions of REE-fluorapatite, REE-fluorite and monazite were received.

Key words: rare earth elements, monazite, apatite, fluorite, thermodynamic modeling, fractionation of lanthanides, fluid

Citation: Kolonin, G. R., G. P. Shironosova (2012), REE distribution coefficients in monazite-fluorite-apatite association depending on HF and *T–P–X* parameters of fluids (thermodynamic modeling), *Vestn. Otd. nauk Zemle, 4*,

Geochemical peculiarities of apatite and monazite composition are actively discussed in literature because they occur widely as accessory minerals. A close association of apatite and monazite is observed. In this case either monazite inclusions are observed in fluorapatite, or fluorapatite crowns sometimes with xenotime and allanite are the result of monazite substitution [*Harlov et al., 2002; Broska et al., 2005; Sindern et al., 2012; Gasser et al., 2012*]. The work [*Harlov et al., 2002*] clearly demonstrates how primarily REE enriched light apatite is converted into the REE depleted dark apatite with monazite inclusions under the action of metamorphosing solutions. The calculation of the ratio between Ce_2O_3 (wt.%) content in these monazite inclusions and Ce_2O_3 content in syngenetic dark apatite shows values of $(0.5–2.0) \cdot 10^3$. This work demonstrates the results of thermodynamic modeling of REE distribution between monazite fluorite and apatite in the temperature interval 500–100°C (the calculation conditions see in Table 1) with the help of HCh computer code [*Shvarov, 1999*]. The influence of the near neutral chloride–carbonate–fluoride solutions on monazite in the presence of calcite has been examined. The detailed description of physical-chemical model and the sources of the initial thermodynamic data are published in our previous paper [*Kolonin, Shironosova, 2011*].

Table 1. P-T-X conditions of thermodynamic calculations

T°C	500	400	300	200	100
P, бар	2000	1000	500	250	125
[NaCl], *m*	4	3.5	3	2.5	2
$[H_2CO_3]$, *m*	1.5	1.25	1	0.75	0.5
[HF], *m*	0.1–0.005	0.1–0.005	0.1–0.002	0.1–0.002	0.1–0.002
$pH_{equilibrium}$	5.9–6.3	5.6–6.0	5.5–5.7	5.8	6.5
$pH_{neutral}$	5.115	5.385	5.43	5.58	6.1

REE-containing minerals are treated in the calculations as ideal solid solutions: monazite ($LnPO_4$), REE-fluorite (CaF_2–(Ln, Y)F_3) and REE-fluorapatite ($Ca_5(PO_4)_3F$–(Ln, Y)$_3(PO_4)_3$), where Ln – La, Ce, Pr, Nd, Sm, Eu, Gd. It should be noted that this association has been obtained in a wide range of the initial HF concentration in the near neutral solutions at 500–300°C, and at 200°C only in the case of solution acidification. The interval of the initial HF concentration at which apatite is stable significantly narrows (0.06–0.002*m*) in the near neutral conditions at 200°C. Fig. 1 demonstrates as an example the diagrams of quantitative relationships of minerals in the equilibrium association at 500, 300 and 100°C. It is clearly seen that at 100°C the apatite stability field becomes narrower and xenotime (YPO4) appears instead of apatite.

When considering the REE distribution in the equilibrium association apatite-fluorite-monazite depending on HF at the constant temperature (diagrams only for 500°C are given as an example – Fig. 2) the stability of the coefficient of distribution between fluorite and apatite is observed only for Ce (diagram **a**). They are about 1800, 50 and 1 at 500, 400 and 300°C, correspondingly. The distribution coefficients of the rest REE under discussion appear to be stable only at high fluorine concentrations in the system (0.1–0.04*m*). Beginning from 0.04*m* HF they monotonously fall as it decreases and only for Nd, Sm (especially at 500°C) and Eu (in the whole temperature interval) the increase of the distribution coefficients in the fluorite/apatite pair is observed. It should be also noted that the dependence curves of distribution coefficients/HF concentration become much more flat as temperature decreases. In this case the distribution coefficients of all lanthanides have value greater than 1, i.e. they prefer to concentrate in fluorite but not in apatite. The distribution coefficients of yttrium are different. They significantly decrease as the initial HF concentration decreases as compared to La, Pr and Gd, but at 300°C become smaller that 1 in the whole interval of HF concentration, this means that yttrium prefers to concentrate in apatite.

The constancy of the distribution coefficients of all REE (from Ce to Gd) between fluorite and monazite within the whole range of HF concentrations is striking (Fig. 2, diagram b). Their values are similar both in the slightly alkaline and weakly acidic medium. The values of coefficients are lower than 1 in all conditions and the decreasing sequence is retained: Gd > La > Pr > Ce > Nd > Eu > Sm. A distinct temperature dependence of REE distribution coefficients between fluorite and monazite is traced (see Table 2.)

Table 2. The values of REE distribution coefficients in fluorite-monazite pair

***T*°C**	**La**	**Ce**	**Pr**	**Nd**	**Sm**	**Eu**	**Gd**
500	0.15	0.025	0.12	0.008	0.002	0.003	0.43
400	0.06	0.008	0.05	0.002	$3·10^{-4}$	$6·10^{-4}$	0.22
300	0.03	0.003	0.02	$5·10^{-4}$	$5·10^{-5}$	$1·10^{-4}$	0.12
$\mathbf{200_{acid}}$	0.008	0.0004	0.005	$8·10^{-5}$	$5·10^{-6}$	$1·10^{-5}$	0.06

REE distribution coefficients in monazite/apatite pair (Fig. 2, diagram c) are significantly higher than 1 and behave similar to the coefficients in fluorite-apatite pair, i.e. they are temperature dependent only at high HF concentrations. The curves of their HF dependencies in the areas of low HF concentrations also flatten as temperature decreases. In this case the distribution coefficients of Sm, Nd and Eu increase as HF concentrations decrease like in the fluorite/apatite pair but unlike La, Pr, and Gd. Ce distribution coefficient is nearly stable and temperature dependent only.

Fig. 3. demonstrates the temperature dependence of weight Ce distribution coefficient between monazite and REE-fluorapatite for three types of solutions: acid

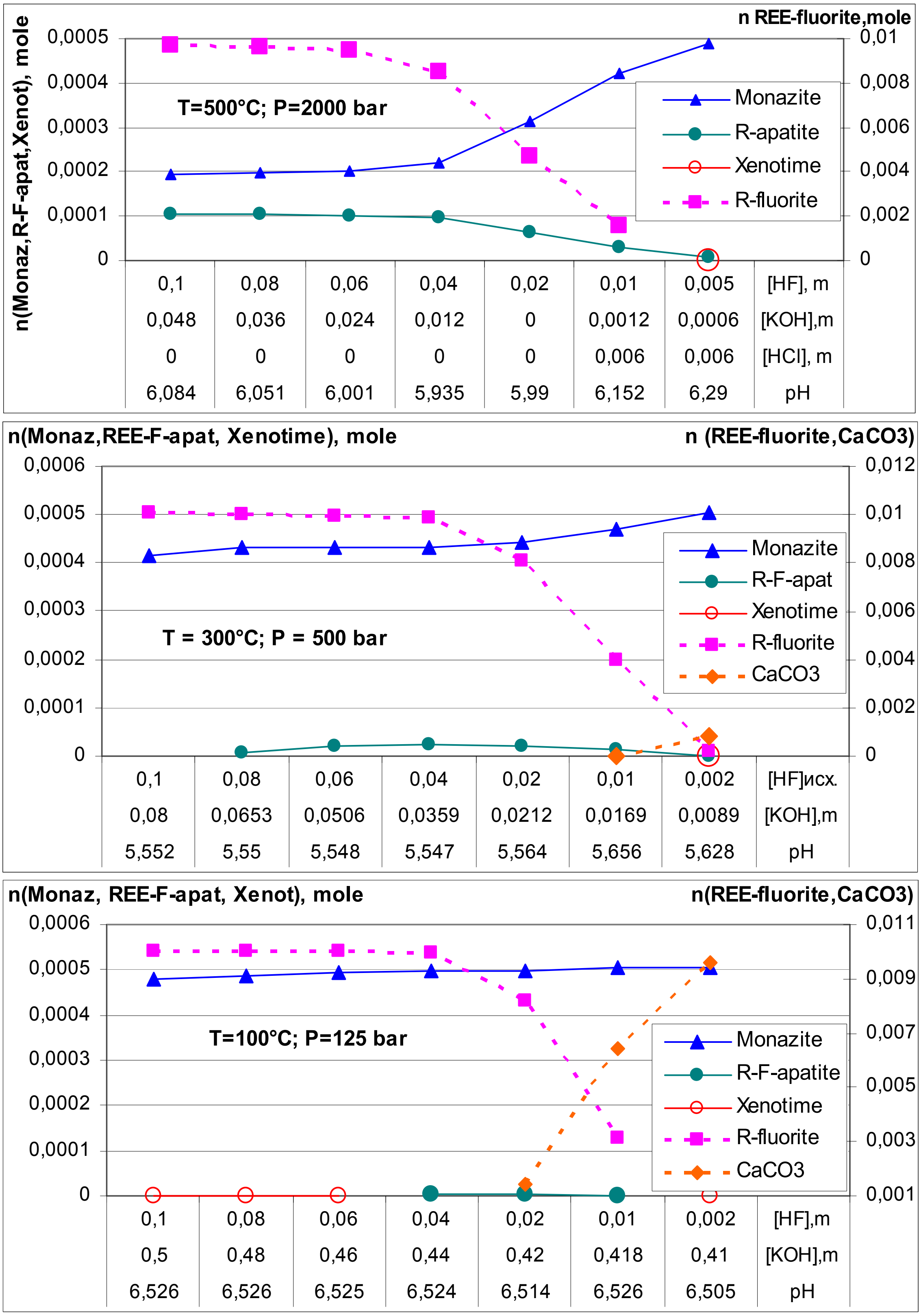

Fig. 1. The influence of the initial HF concentration on the phase composition in REE-fluorite–REE-fluorapatite–monazite equilibrium association during cooling of the system in the temperature interval 500–100°C

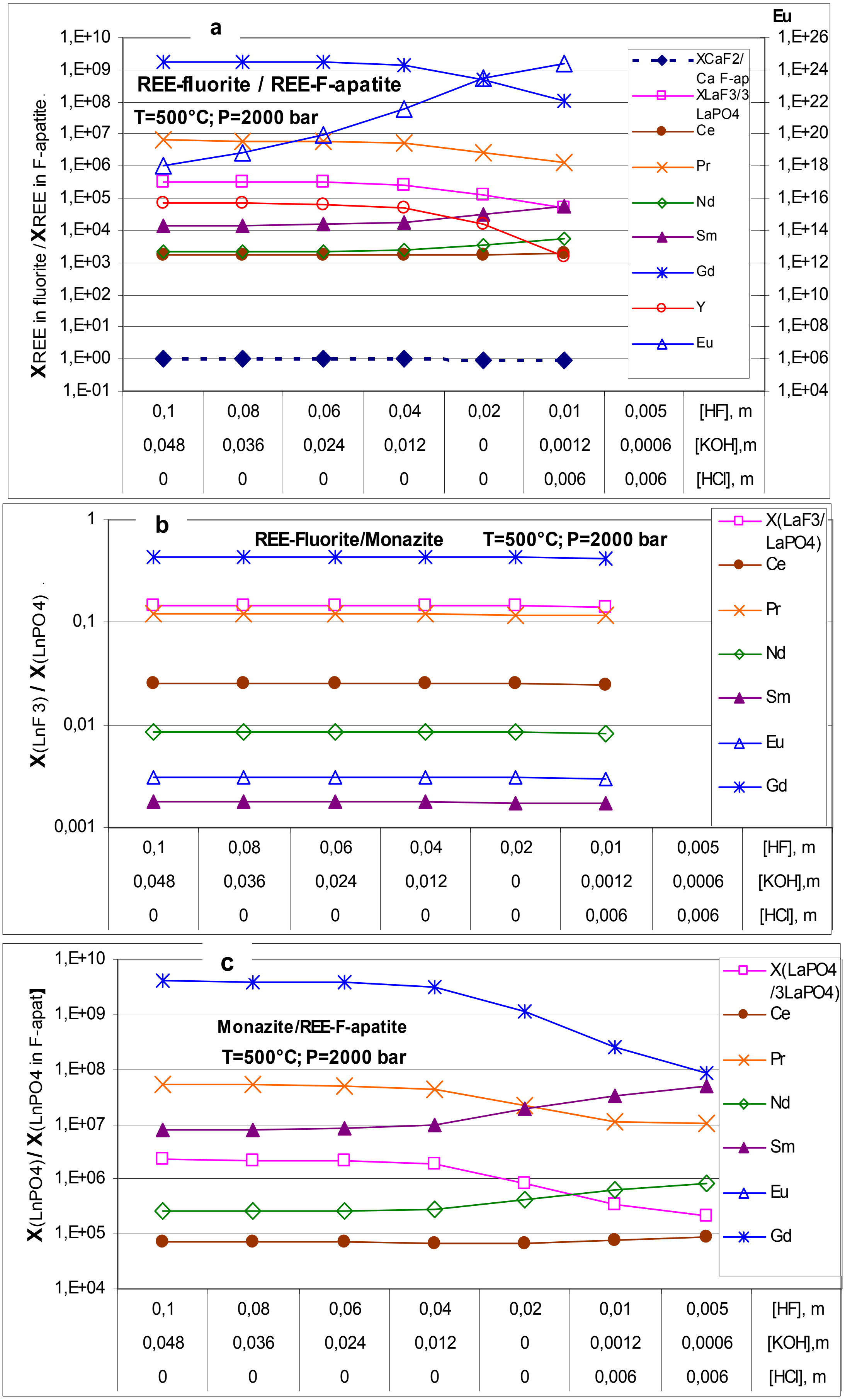

Fig. 2. The influence of the initial HF concentration on REE distribution coefficients in REE-fluorite–REE-fluorapatite–monazite equilibrium association at 500°C and 2000 bar; X – mole fraction of the corresponding component

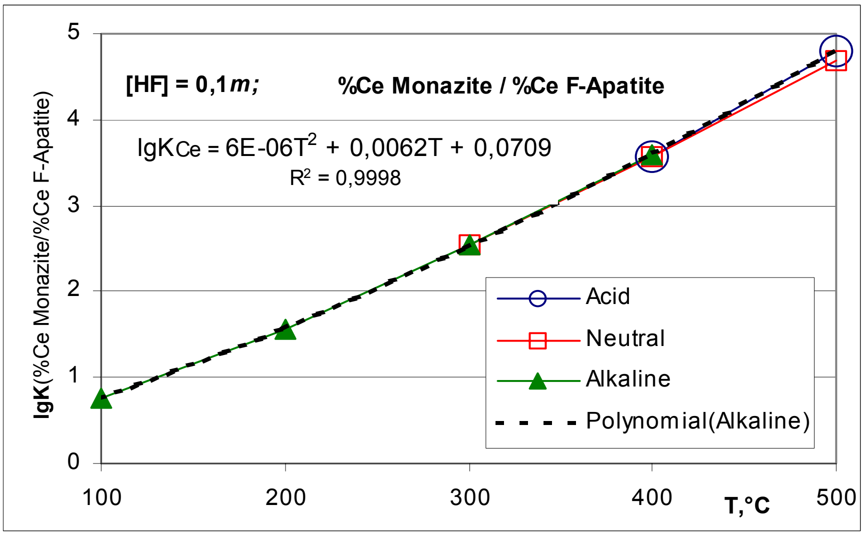

Fig. 3. Temperature dependence of weight Ce distribution coefficient between monazite and REE-fluorapatite for acid, near neutral and alkaline solutions

with pH 4.7, near neutral – 7.1 and alkaline – 8.2. The second-degree equation describes well the data for acid and alkaline solutions and slight deviation is observed only for near neutral solution at 500°C. Thus, cerium distribution between the minerals of apatite-fluorite-monazite equilibrium association can be an indicator temperature of its formation.

The work is supported by RFBR, grant N 11-05-00662

References:

1. Broska, I., C. T. Williams, M. Janak, G. Nagy, G. (2005), Alteration and breakdown of xenotime-(Y) and monazite-(Ce) in granitic rocks of the Western Carpathians, Slovakia, *Lithos*, Vol. 82, pp. 71–83.
2. Gasser, D., E. Bruand, D. Rubatto, K. Stuwe (2012), The behavior of monazite from green schist facies phyllites to anatectic gneisses: An example from the Chugach Metamorphic Complex, southern Alaska, *Lithos*, Vol. 134-135, pp. 108–122.
3. Harlov DE., U.B. Andersson, H-J. Forster, J.O. et al. (2002), Apatite–monazite relations in the Kiirunavaara magnetite–apatite ore, northern Sweden, *Chemical Geology*, Vol. 191 pp. 47–72.
4. Kolonin, G. R., G. P. Shironosova (2011), The dependence of monazite composition on HF concentration and T-PX parameters of fluids (thermodynamic simulation), *Vestn. Otd. nauk Zemle*, 3, NZ6037, http://onznews.wdcb.ru/publications/v03/asempg11en/2011NZ000167.pdf
5. Shvarov Yu. V. (1999), Algorithmization of the numeric equilibrium modeling geochemical processes, *Geochemistry International* No. 6, 571–576.
6. Sindern S., A. Gerdes, Yu. L. Ronkin, et al. (2012), Monazite stability, composition and geochronology as tracers of Paleoproterozoic events at the eastern margin of the East European Craton (Taratash complex, Middle Urals), *Lithos*, Vol. 132-133, pp. 82–97.

Korzhinskaya V.S. Effect of physico-chemical conditions on pyrochlore solubility in fluoride solutions at T = 300–550oC and P = 500–1000 bar

Institute of Experimental Mineralogy RAS vkor@iem.ac.ru

Experimental studies on pyrochlore solubility in HF and KF solutions are continued. It is determined that pyrochlore has a weakly marked temperature dependence in HF and a strongly marked one in KF solutions. The dependence of mineral solubility on HF and KF concentrations is strong, positive. The influence of redox conditions in the limits of Ni–NiO and Co–CoO buffers is almost negligible. The role of temperature, pressure and redox conditions for this type of deposits is secondary.

Key words: experiment, pyrochlore, columbite, solubility, buffer, fluorine.

Citation: Korzhinskaya V.S. (2012). Effect of physico-chemical conditions on pyrochlore solubility in fluoride solutions at T=300–550C and P=500–1000 bar, *Vestn.Otd. nauk Zemle,* 4

We carry out systematic investigations of solubility of mineral phases of tantal-niobates of a complicated compositon stable under natural conditions (columbite, pyrochlore etc.). Earlier we studied the behavior of columbite-tantalite in fluoride and chloride solutions what is important for tantal and niobium deposits, connected with lime-alkaline, including lithium-fluorine granites ("apogranites"). [*Zaraisky G.P.,Korzhinskaya V., Kotova N., 2010*]. It has been shown that participation of acidic fluoride solutions of high concentration (1.0m and higher) and redox situation are favourable for a hydrothermal transfer of Ta and Nb. For the first time established a strong increase of tantal-columbite solubility (by 1.5–2 orders of magnitude) with the decrease of oxygen fugacity from the Ni-NiO level to the Co-CoO buffer can be extremely important to form this type of deposits in "apogranites" due to high reduction of high-temperature magmatogeneous aqueous fluids, generated by the maternal granites of the "ilmenite type". A subsequent increase of oxygen fugacity on the postmagmatic stage in the domes of rare-metal granites can serve one of the main reasons of tantal-niobate deposition here. Experimental investigations of the behavior of pyrochlore $(Ca,Na)_2$ $(Nb,Ta)_2O_6$ (O,OH,F) and columbite (Mn,Fe) $(Nb,Ta)_2O_6$ in sodium carbonate and alkaline solutions typical for the deposits of these metals genetically connected with alkaline granites, alkaline sienites and carbonatites are also carried out [*Korzhinskaya V. S., Zaraisky G. P., 2008a; Korzhinskaya V. S., Zaraisky G. P., 2009*].

These data are a continuation of the experimental study on the solubility of natural pyrochlore $(Ca,Na)_2(Nb,Ta)_2O_6(O,OH,F)$ in HF and KF solutions. Temperature dependence of pyrochlore solubility for 300, 400, 500 and 550°C is obtained at pressures 500 - 1000 bar and oxygen fugacity corresponding to the buffers Ni–NiO and Co–CoO. Thus, the whole spectrum of the conditions of formation of tantal-niobium deposits in different solutions within a wide range of change of concentration, temperature, pressure and oxygen fugacity will be involved into the runs.

A monocrystal of pyrochlore was selected from was selected from weathering crusts of carbonatite deposit Tatarka of the following composition: Na_2O – 7.61%; CaO – 14.28%; Nb_2O_5 – 71.61%; F – 5.18%; TiO_2 – 0.83%; $Ta_2O_5 \leq 1\%$ wt. The concentration of the solutions HF and

KF varied in the limits 0.01–2m. The preliminarily weighed fragment of the monocrystal was placed at the bottom of the platinum capsule of 10x 0,2x60 mm in size, was flooded by the solution of 1 ml. The run duration was 15 to -20 days. The experiments were carried out in platinum capsules of the hydrothermal exoclave high pressure vessel in the presence of containers with solid-phase oxygen buffers (Ni-NiO, Co-Co) isolated from the charge. A quenching solution was analyzed by ICP/MS and ICP/AES (mass-spectral and atomic-emission) methods for a row of elements (Nb, Ta, Na, Ca, Mn, Fe, Ti etc.). A solid charge was analyzed by the x-ray and microprobe methods.

Experimental data are shown in Figs. 1–6. The data showed that pyrochlore dissolves in HF and KF incongruently [*Korzhinskaya V.S, 2011*]. Fig.1 shows temperature dependence of pyrochlore solubility in HF solutions. According to our experimental data over all investigated range of temperatures and concentrations the temperature dependence of the solubility of pyrochlore is weakly expressed. Here concentration dependence is positive. With the growth of HF concentration from 0.10 m to 2m the niobium content in the solution increases from n*10^{-6} mol/kg H_2O for 0,01m solution to n* 10^{-1} mol/kg H_2O–for 2m HF. For KF solutions temperature dependence is positive (Fig.3) but concentration dependence (Fig.2) is expressed less markedly than for HF solutions. With the growth of KF concentration from 0,01m to 1 m the Nb content increases only by 1–1.5 orders.

Fig.2 shows concentration dependence of pyrochlore solubility in HF and KF solutions at P=0.5 and 1 kbar. It is determined that in HF and KF solutions the dependence of pyrochlore solubility on pressure is positive. At high concentrations of fluoride (1 and 2 m) and P = 1000 bar the Nb content is half an order higher than at P = 500 bar. At low concentrations of HF and KF (0.01m–0.5m) no pressure effect can be seen.

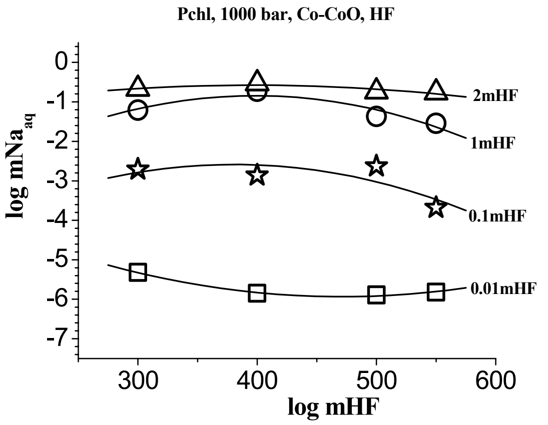

Fig. 1. Temperature dependence of pyrochlore solubility in HF solutions at P = 1000 bar (Co–CoO buffer)

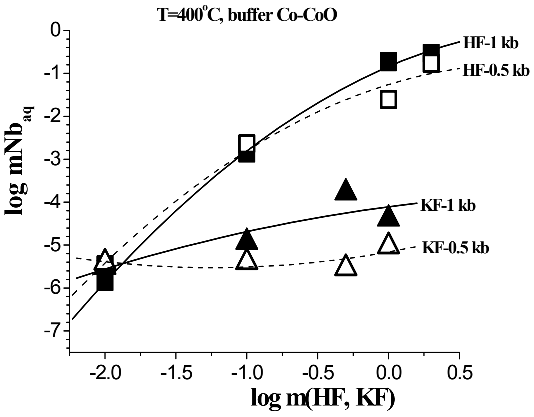

Fig. 2. Concentration dependence of pressure effect on pyrochlore solubility in HF and KF solutions at T = 400°C (Co–CoO buffer)

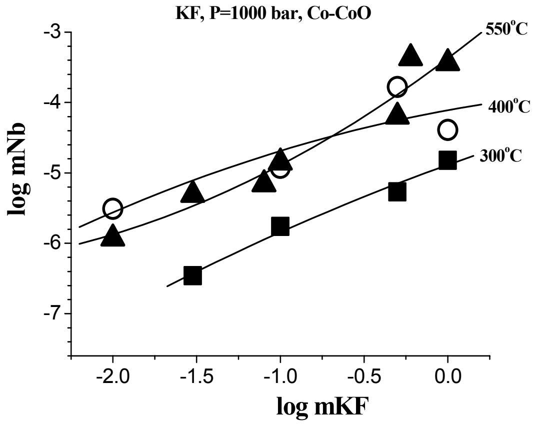

Fig. 3. Concentration dependence of pyrochlore solubility in KF solutions at T=300, 400 and 550°C and P = 1000bar (Co–CoO buffer)

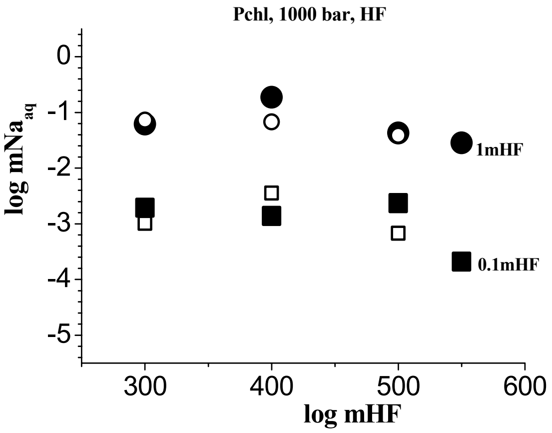

Fig. 4. Temperature dependence of pyrochlore solubility in HF solutions for different redox conditions (white symbols - Ni–NiO buffer; - dark symbols Co–CoO buffer)

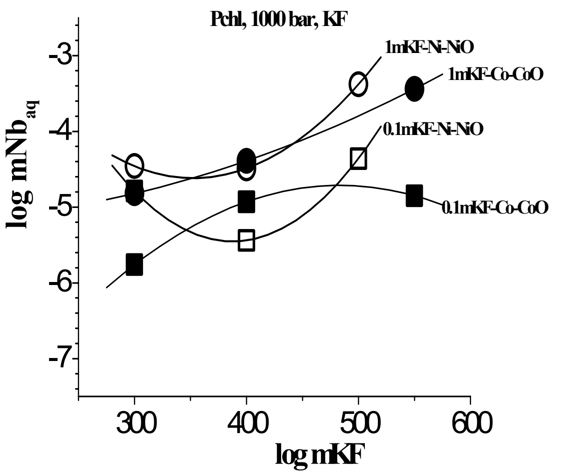

Fig. 5. Temperature dependence of pyrochlore solubility in KF solutions for different redox conditions (white symbols – Ni–NiO buffer; dark symbols – Co–CoO buffer).

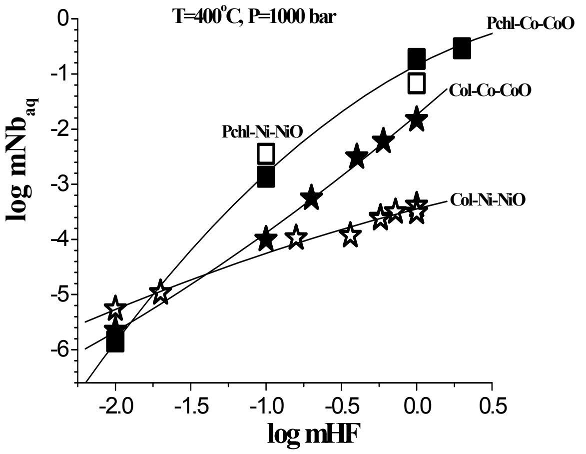

Fig. 6. Concentration dependence of columbite and pyrochlore solubility in HF solutions under different redox conditions (white symbols – Ni–NiO buffer; dark symbols – Co–CoO buffer)

Earlier, it has been shown that the solubility of columbite-tantalite is 1.5 to 2 orders of magnitude higher under more reducing conditions (buffer Co-CoO) than under more oxidizing conditions (buffer Ni-NiO) [*Korzhinskaya V.S., Zaraisky G.P. 2008b*]. To clarify the effect of redox conditions on natural pyrochlore (Ca, Na)$_2$(Nb, Ta)$_2$O$_6$(O, OH, F) solubility in HF and KF solutions we performed a series of the experiments with the concentrations 0,1 and 1,0 mol/kg H_2O at T = 300–550°C, P = 1000 bar in the presence of the Co–CoO and Ni–NiO oxygen fugacity buffers. Fig.4 and Fig.5 show temperature dependence of pyrochlore solubility in HF and KF solutions with the concentrations 0.1m and 1m buffered either to the Ni–NiO or Co–CO oxygen fugacity buffer. The effect of the redox conditions in the limits of the Ni–NiO and Co–CoO buffers is practically not seen in HF solutions. For KF solutions the picture is somewhat different (Fig.5). At T = 400°C the Nb concentraton in 1m KF buffered to the Ni-NiO oxygen fugacity buffer is a bit lower and in 0.1m KF more than by 0.5 order lower. At T = 500°C, on the contrary, the Nb content under Ni–NiO oxidizing conditions is half an order higher than under Co–CoO reducing conditions. Fig.6 shows the comparative data of Nb content in HF solutions for natural minerals of pyrochlore and columbite. As we see the columbite solubility under reducing conditions (Co–CoO buffer) is more than by 2 orders of magnitude than that under Ni–NiO oxidizing conditions. Metals Mn and Fe changing their valence with changing redox conditions enter columbite composition.

On the basis of the obtained experimental data one can conclude that pyrochlore and columbite solubility in fluoride solutions is rather high. That allows us to speak about a possibility of real Nb transfer via concentrated fluoride solutions (HF and KF). It is concluded that the deposition of niobium favors reducing the concentration of fluoride. The role of temperature, pressure and redox conditions for this type of deposits is secondary.

Financial support by RFBR, project 10-05-00292-a.

References :

1. Korzhinskaya, V. S. (2011). Experimental study of dependence of pyrochlore solubility in HF and KF solution at T= 400°, 550°C and P = 1000 bar, *Vestn. Otd. nauk Zemle, 3*, NZ6042, doi:10.2205/2011NZ000172.
2. Korzhinskaya, V. S., G. P. Zaraisky (2008a). Experimental study of concentration dependence of pyrochlore and columbite solubility in carbonate solutions at T = 550°C and P = 1000 bar. *Vestn. Otd. Nauk Zemle RAN,* №1 (28)`2008, Moskow, IPE RAS.
3. *URL: http://www.scgis.ru/russian/cp1251/h_dgggms/1-2008/informbul-1_2008/hydroterm-15.pdf*
4. Korzhinskaya, V. S., G. P. Zaraisky (2009). Experimental study of concentration dependence of pyrochlore and columbite solubility in NaOH solutions at T = 550°C and P = 1000bar. *Vestn. Otd. Nauk Zemle RAN,* №1 (27)`2009, Moskow, IPE RAS.
5. *URL: http://www.scgis.ru/russian/cp1251/h_dgggms/1-2009/informbul-1_2009/hydroterm-15e.pdf.*
6. Korzhinskaya, V. S., G. P. Zaraisky (2008b). Experimental study of physico-chemical conditions influence on tantalite-columbite solubility in hydrothermal fluids. In: Granites and Earth evolution: geodynamic position, petrogenesis and ore-bearing of granitoid batolites. Proceedings of the I-st international geological conference. Ulan-Ude. Buryatskii research centre Rus.Acad.Sci, p. p.193–195.
7. Zaraisky, G. P., V. Korzhinskaya, N. Kotova (2010). Experimental studies of Ta_2O_5 and columbite-tantalite solubility in fluoride solutions from 300 to 550°C and 50 to 100 MPa, *Miner. Petrol.*, v. 99, № 3-4, p.p. 287–300.

Korzhinskaya V.S., Kotova N.P. Experimental modeling of possibility of hydrothermal transferring niobium by fluoride

Institute of Experimental Mineralogy RAS *vkor@iem.ac.ru*; *kotova@iem.ac.ru*

Concentration dependence of Nb_2O_5 and natural columbite and pyrochlore solubility is studied in HF and KF solutions in a wide range of concentrations 0.01m–2m at T = 550°C, P = 1000bar and under Co-CoO oxidizing conditions. It is determined that in HF and KF solutions a positive concentration dependence of Nb solubility both for natural minerals of columbite and pyrochlore and for Nb_2O_5 is observed, attaining n*$10^{-0.5}$ m for Nb_2O_5 and pyrochlore and n*10^{-2} m – for columbite. The similar picture is observed in KF solutions. The obtained data confirm the thesis that solubility of simple oxides (Ta_2O_5 and Nb_2O_5) restricts the upper limit of concentration of these elements in the hydrothermal solutions.

Key words: experiment,, pyrochlore, columbite, Ta and Nb oxides, solubility, fluoride solutions

Reference: Korzhinskaya V.S., N.P. Kotova (2012), Experimental modeling of possibility of hydrothermal transferring niobium by fluoride *Vestn.Otd. nauk Zemle,*

Metasomatic origin of W, Mo, Sn, Be and Bi greisen deposits connected with both leucocrate and lithium-fluoride granites is practically not disputed by anybody. However, with respect to Ta, Nb, Li and other rare metals associating with them many geologists consequently prove the ideas on a magmatic origin of rare-metal Li-F granites and the leading role of magmatic processes of crystallization differentiation of the melt in concentrating Ta, Nb, Li, Rb, Be, Zr, Th and other rare elements. Modern ideas on belonging "apogranites" to Li-F type of granite rocks are connected with the works of V.I. Kovalenko et al, proving their magmatic genesis for many years [*Kovalenko, 1977*]. It has been determined that in the process of deep fractioning of granite magma up to the level of ongonites and lithium-fluorine granites in the residual melts there occurs a considerable accumulaion of F, Li, Ta, Nb and some other rare metals which minerals get a chance to be crystallized from the melt in the form of a fine accessory embedding. At present this viewpoint has become dominant in the world science. However, the appearance of even a poor accessory embedding and other tantal-niobates in the intergrain space of Li-F granites has principal importance since it makes possible a subsequent mobilization, transfer and redeposition of Ta and Nb by a hydrothermal fluid. Further concentration of Ta and Nb up to the economically significant quantities seems to occur by a hydrothermal-metasomatic way during greisenization and albitization of granites by flows of postmagmatic fluoride fluids with the redeposition of tantal-niobates in the upper part of domes of Li-F granites under the screen of metamorphosed to hornfels schiested roof. So far such a possibility has never been proved experimentally by anybody. In literature reliable data on the behavior of Ta and Nb under hydrothermal conditions have been absent. The solution of this problem needed special experimental investigations under the conditions of temperatures, pressures and compositions of the solutions corresponding to physico-chemical parameters of postmagmatic processes in the domes of lithium-fluorine granites.

Earlier we have carried out the experiments on determination of the behavior of columbite-tantalite and tantalum oxide in fluoride, chloride and carbonate solutions. It has been proved for the first time that Ta and Nb can be transferred by a hydrothermal way and be deposited in the form of proper minerals. However, in carbonate and chloride fluids the Ta and Nb solubility is negligible. So one can say about a real transfer of Ta and Nb by high concentrated fluoride solutions only, mainly by HF and KF [*Zaraisky G.P., Korzhinskaya V., Kotova N., 2010*].

We have studied the effect of the presence of small amounts of F^-- ions to be introduced as NaF, the solubility of pyrochlore and niobium oxide solubility in the solutions of Na_2CO_3+NaF and NaOH+ NaF. Here we determined its positive influence on solubility of tantal-niobates in neutral and carbonate solutions. The participation of fluorine in the processes of mineral formation on Ta and Nb deposits of alkaline type is proved by the presence in ores of these deposits of fluorite, cryolite, villiomite as well as its entering micas, amphiboles, pyrochlores, apatites and other minerals.

This study is a continuation of systematic experimental investigations on solubility, transfer and deposit of minerals of Ta and Nb by hydrothermal fluids. This study gives experimental investigations of behavior of pyrochlore ($(Ca, Na)_2(Nb, Ta)_2O_6(O, OH, F)$, columbite $(Mn, Fe)(Nb, Ta)_2O_6$ and Nb oxide (Nb_2O_5) – the analogue of natural mineral of nioboxide in fluoride solutions:HF and KF.

Concentration dependence of natural columbite, pyrochlore and Nb oxide solubility is studied in HF and KF solutions in a wide range of concentrations 0.01–2 m at T = 550C, P = 1000 bar and low oxygen fugacity (Co–CoO buffer). The experiments have shown that within the wide range of concentrations HF and KF pyrochlore and niobium oxide dissolve incongruently with the formation of new phases. Congruent solubility in HF is observed for columbite and the incongruent one can be seen in KF solutions [*Zaraisky G.P., Korzhinskaya V., Kotova N., 2010*].

For HF and KF solutions we see positive concentration dependence of the Nb solubility both for natural minerals of columbite, pyrochlore and for Nb_2O_5 (Figs.1, 2).

Fig. 1 shows concentration dependence of solubility of pyrochlore, columbite and Nb_2O_5 in HF solutions.

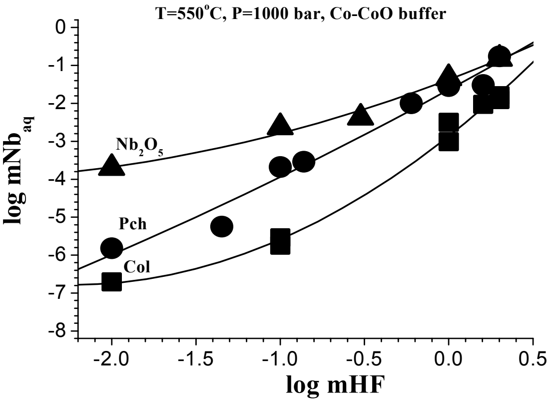

Fig. 1 Concentration dependence of niobium oxide, pyrochlore and columbite solubility in HF solutions at T = 550°C, P = 1000 bar (Co-CoO buffer)

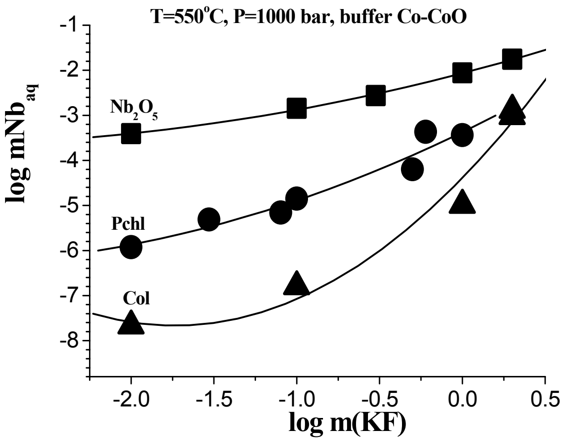

Fig. 2 Concentration dependence of niobium oxide, pyrochlore and columbite solubility in KF solutions at T = 550°C, P = 1000 bar (Co-CoO buffer)

It is found that in HF solutions at low concentrations (0.01m) the niobium content is maximum for Nb_2O_5 and is $n*10^{-4}$ m; for pyrochlore it is $n*10^{-6}$ m, but for columbite it is $n*10^{-7}$ m. At high concentrations of HF (1.0 m and higher) the niobium content increases, reaching $n*10^{-0.5}$ m for Nb_2O_5 and pyrochlore and $n*10^{-2}$ m – for columbite.

Fig. 2 shows concentration dependence of pyrochlore, columbite and Nb_2O_5 solubility in KF solutions. It can be seen from Fig. 2 that at low concentrations of KF (0,01 m) the niobium content is maximum for Nb_2O_5 and is $n*10^{-3.5}$ m; for pyrochlore it is $n*10^{-6}$ m , but for columbite it is $n*10^{-7.5}$ m. At high concentration of KF the niobium content is maximum for Nb_2O_5 ($n*10^{-2}$ m), but for pyrochlore and columbite it has the similar values and is $n*10^{-3.5}$ m. The obtained data confirm the thesis that solubility of simple oxides (Ta_2O_5 and Nb_2O_5) restricts the upper limit of concentration of these elements in hydrothermal solutions.

From the obtained data on solubility of natural columbite, pyrochlore and Nb oxide solubility in fluoride solutions consisting of HF and KF at T=550C, P=1000bar we can conclude that pyrochlore dissolves much better than columbite in both HF and KF solutions. Its solubility is 1–1.5 orders of magnitude higher at of low fluoride concentrations. Solubility of Nb oxide in HF solutions at low concentrations is approximately an order and a half higher than that of natural minerals, but in KF solutions the niobium content for Nb oxide is 2.5–3.5 orders of magnitude higher than for pyrochlore and columbite. At fluoride concentrations of 1-2m the niobium and natural minerals solubility increase markedly and become approximately comparable.

Experimental results can serve an objective basis to estimate the possibility of Nb mass transfer by hydrothermal solutions in natural conditions since on the basis of the obtained concentration curves we can judge about the maximum possible value of the Nb concentration in an aqueous fluid at the early postmagmatic stage after its separation from the crystallizing granite melt. The obtained data clearly show that participation of acidic fluoride solutions, high concentration of fluorine and redox conditions are favourable for Nb solubility and transfer (as well as for Ta) by aqueous fluids. The sedimentation of Ta and Nb minerals from the solutions with the formation of their deposits can take place as a result of (1) neutralization of acidic fluoride solutions (2) the decrease of fluorine concentration and (3) the increase of oxygen fugacity.

Financial support by RFBR, project 10-05-00292-a; 11-05-01185-a.

References :

1. Kovalenko, V. I. (1977). Petrology and Geochemistry of Rare-Metal Granitoids (Nauka), Novosibirsk, (in Russian).
2. Zaraisky, G. P., V. Korzhinskaya, N. Kotova (2010). Experimental studies of Ta_2O_5 and columbite–tantalite solubility in fluoride solutions from 300 to 550°C and 50 to 100 MPa, *J. Mineralogy and Petrology*, № 99, pp. 287–300.

Koshcheeva I.Ya., Tyutyunnik O.A., Chkhetia D.N., Krigman L.V., Kubrakova I.V. Role of natural organic substances in colloidal transport of platinum and palladium

V. I. Vernadsky Institute of Geochemistry and Analytical Chemistry RAS, Moscow kubrakova@geokhi.ru, NMlab@geokhi.ru

In order to study a migration behavior of platinum group metals (PGM) in natural water systems, the sorption of dissolved chloro- and hydroxochloro complexes of platinum (IV) and palladium (II) by major components of suspensions and bottom sediments (humic acids, iron oxyhydroxides (FeOOH) and aluminosilicates (clay shale and klynoptilolite)) – under conditions typical for surface fresh waters has been investigated. The distribution of platinum and palladium between a solution and suspended matter in real colored river waters has been studied.

Key words: platinum, palladium, migration behavior, natural water systems

Citation: Koshcheeva, I. Ya., O. A. Tyutyunnik, D. N. Chkhetia, L. V. Krigman, I. V. Kubrakova (2011), Role of natural organic substances in colloidal transport of platinum and palladium, *Vestn. Otd. nauk Zemle,* 4

Kotelnikov[1] A.R., Suk[1] N.I., Kotelnikova[2] Z.A., Tschekina[3] T.I., Kalinin[1] G.M. Mineral geothermometers for low temperature paragenesis

[1]Institute of Experimental Mineralogy RAS, Chernogolovka kotelnik@iem.ac.ru
[2]Institute of Geology of Ore Deposits, Petrography, Mineralogy, and Geochemistry, RAS, Moscow
[3]M. V. Lomonosov Moscow State University, Department of Geology, Moscow

The experimental study of chlorite geothermometer based on alumina distribution between nonequivalent structural positions [*Cathelineau & Neiva, 1985*] was carried out at temperature 200 – 250°C; P=0.5 kbar under hydrothermal conditions. A good correspondence of our experimental results and empiric data of [*Cathelineau & Neiva, 1985*] was demonstrated. The experimental study of albite ordering processes was carried out at 200–500°C, P=0.5–1.0 kbar. The special equation for temperature estimation using odering parameter Δ131was calculated. The temperatures of mineral genesis of paleovolcanic rocks were estimated using albite ordering thermometer, chlorite thermometer and data of fluid inclusions study.

Key words: chlorite, albite, alumina distribution between structural positions, fluid inclusions, temperatures of mineral genesis

Ref: Kotelnikov A. R. , V. V. Ananiev, N. I. Suk, G. M. Akhmedjanova (2012), Mineral geothermometers for low temperature paragenesis, *Vestn. Otd. nauk Zemle, 4,*